The method of 3D reconstruction of apple shape. Part 1. Apple shape mathematical modeling method

LESZEK MIESZKALSKI
Department of Production Management and Engineering, Warsaw University of Life Sciences – SGGW

Abstract: *The method of 3D reconstruction of apple shape. Part 1. Apple shape mathematical modeling method*. This work presents a proposed method for mathematical modeling of apple shape using Bézier curves. The apple contour on its meridian has been described by three connected Bézier curves. The basis for description of apple contours using Bézier curves are photographs of an apple, rotated every 36° with reference to its natural axis of symmetry. Bézier curves along the apple's meridians constitute its 3D model. Bézier curves were used to describe the shape of the seeds the chamber and seed nest of the apple.

Key words: apple, seeds the chamber, seed nest, shape, Bézier curves, method, mathematic model

INTRODUCTION

Rogge et al. [2014] used the computer tomography of quasi-axisymmetric biological objects for modeling of apple shape. X-ray images were used to determine the apple contours, which served as a basis for specification of shape descriptors. Elliptic Fourier descriptors were used for the purpose. Afterwards, using the reverse descriptor transformation through interpolation and geometric transformation [Foley et al. 2001, Kiciak 2000], geometric 3D models of apples were obtained. Mebatsion et al. [2011] proposed a procedure for description of the shape of symmetric fruit using the longitudinal contours, described by Fourier descriptors using algorithms to smooth the surface of the fruit or vegetable.

Abera et al. [2014] developed a 3D generator to model fruit tissue. The model was based on biomechanics of cells, in which cellular walls are modeled as elastic components. The virtual model of fruit tissue takes into account the cell shape and intracellular space, and it can be used to model physical processes taking place in fruit cells and tissues. Goñi et al. [2008] used the magnetic resonance technique to model geometry of food materials. The contours of cross--sections of the objects examined were described by B-splines. The 3D model was built using the Lofting method through interpolation of B-splines. Goñi and Purlis [2010] modeled geometry of internal tissues of food materials using the color segmentation technique, applying the distance criterion, and the model was developed through linear interpolation. Ho et al. [2013] are of opinion

that large scale modeling would allow for describing of behavior of biological materials at various spatial scales, with the possibility of putting together the fragments of micro structure images. Kakadiya et al. [2015] and Moreda et al. [2012] believe that the shape of biological objects is their key property. According to Costa et al. [2011], shape plays an important role in fruit assessment, classification and sorting using vision systems. Image processing algorithms are widely used for measurement of external geometric properties. Fruit quality assessment systems, according to Pandey et al. [2013], should employ many classification tools, such as: geometric image analysis, color, fractal techniques, classifier correlation with fruit quality. Liming and Yanchao [2010] proposed an automated strawberry fruit classification system, based on such features as shape, dimensions and color. Applying the decision-making theory, a high level of assessment accuracy was achieved: error in strawberry size recognition was 5%, color recognition accuracy – about 89%, and shape recognition accuracy – 90%. Prusinkiewicz and Runions [2012] proposed a plant shape development calculation method.

Hazbavi [2014] determined the maximum height of box of apples stored in a rectangular-shaped container. He assumed the spherical apple shape for the purpose of his calculations. He calculated the diameter of the sphere, being the apple model, as the geometric average

on the basis of measurement of the apple length, width and thickness. Torabi et al. [2013] modeled apple volume on the basis of its comparison with regular-shaped solids, such as oblate spheroid and ellipsoid, obtaining, as they claim a very high matching level (0.95–0.98). To model apple mass, Chakespari et al. [2010] also used the ellipsoid and oblate spheroid. According to Arshad et al. [2014], physical properties of apples are of fundamental significance during harvest and mass processing, and, in particular, in designing of processing machines and equipment. Among the numerous physical properties, the size, shape, surface and color are of significance when making decisions at various stages of production and processing of apples. Bakane et al. [2014], apart from dimensions, point out other physical properties of apples, such as: actual density, bulk density, pile porosity, chute angle and friction coefficient.

Uyar and Erdoğdu [2009] applied the 3D scanning technique to describe fruit shape. The technique of 3D scanning of biological objects using a scanner requires many scans, which can be used to come up with a model of a single object (Fig. 1). Anders et al. [2014] produced nine partial scans for each fruit. The author of this work managed to generate an apple model using six partial scans (Fig. 1). The need to combine a solid using many scans with markers should be considered a flaw of the method.
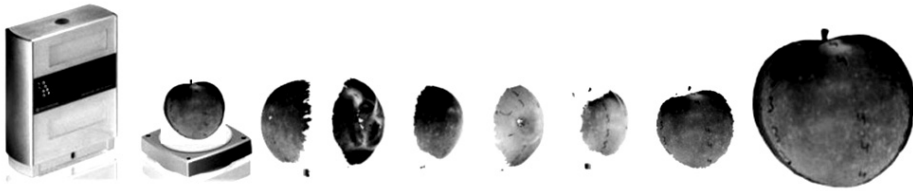
FIGURE 1. Exemplary 3D scans of apples using a Nextengine scanner
Source: Own compilation.

The stock management methods used by production and trade companies [Buliński et al. 2012, 2013], as well as the classificatin and diagnostics methods [Janaszek and Trajer 2010] make it possible to identify the properties, which influence the product quality. Use of computer tomography (CT) and magnetic resonance (MRI) methods to obtain apple images requires substantial financial expenditures. Therefore, it is necessary to develop simple and cheap methods of 3D shape reconstruction, which will generate sufficiently accurate data on the apple being modeled.

This work presents the proposed method for mathematical modeling of apple shape using Bézier curves.

MATERIAL AND METHODS

Jonagored apples, characterized by substantial size and shape similar to a wide cone can be used for direct consumption and processing and stored in a refrigeration plant. After purchase at the warehouse in Bronisze, apples were stored in a room of constant temperature of 19°C and air humidity of 60%. From a set of 50 apples, one undamaged apple of medium size was selected for modeling.

The apple, in its natural axis of symmetry, was placed on the stand (Fig. 2) for the purpose of making photographs in 10 positions obtained by rotating the apple every 36°. The natural axis of
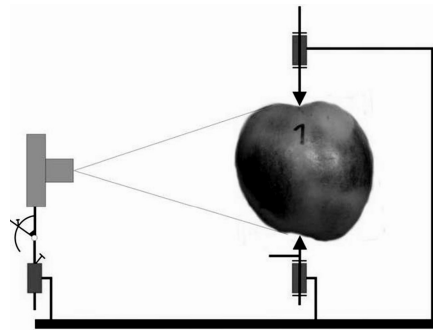

FIGURE 2. The test stand
Source: Own compilation.

symmetry of the apple is the line connecting the stem cavity with the pistil cavity. The photograph was made using Panasonic LUMIX DMC-TZ3. The distance between the lens and the object was constant and amounted to 400 mm. Photographs of dimensions of 2,560 × × 1,712 pixels were saved in JPEG format. The shape of contours of the seeds the chamber and seed nest were determined after cutting the apple. The basic dimensions of the apple (length, width

and thickness, as well as h_1 and h_2) illustrated by Figure 3 were measured with a slide caliper with accuracy up to 0.1 mm. The apple length was $h =$ $= 77.8$ mm, width $\varphi a = 84.1$ mm, thickness $\varphi b = 82.6$ mm, while dimensions $h_1 =$ $= 15.1$ mm and $h_2 = 13.9$ mm.

ed Bézier curves and two Bézier curves for both the contours of the seeds the chamber and the seed nest (Fig. 4). The starting point of the coordinate system was within the symmetry axis of the apple, while the x axis was adjacent to the lower part of the fruit. The apple is
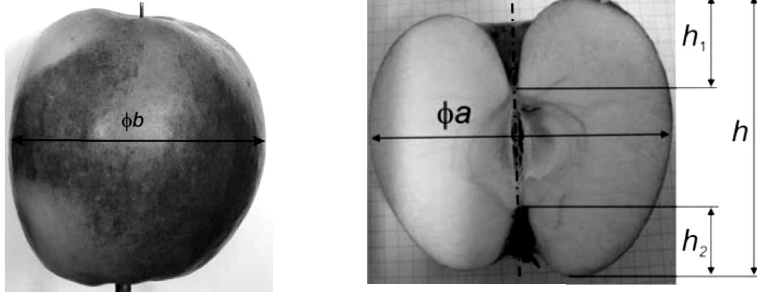

FIGURE 3. Jonagored apple selected for modeling and the basic dimensions of its cross-section and the natural axis of symmetry
Source: Own compilation.

The framed photograph of the apple was loaded to graphic software, such as Inkscape, and placed in a coordinate system. After scaling the apple, its contours were matched with three connect-

a solid with a concavo-convex surface. It was necessary to use h_1 and h_2 values to determine the position of nodal points Ax, Ay, Az, Cx, Cy, Cz of Bézier curves (Fig. 4).
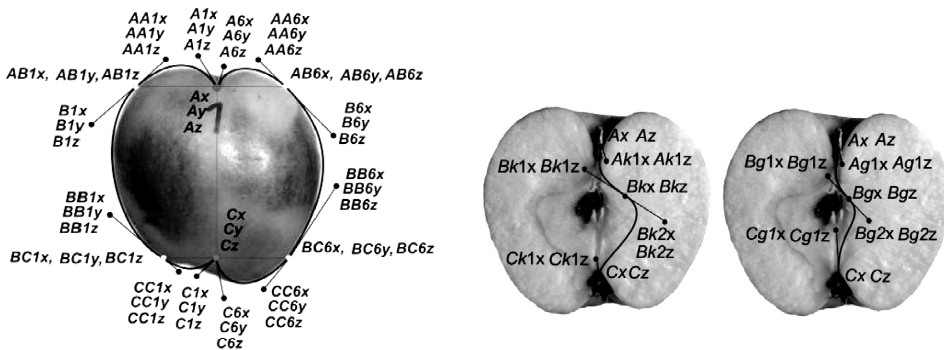

FIGURE 4. Marking of nodal points and control points of three Bézier curves describing the apple contour, two Bézier curves describing the seeds the chamber and two Bézier curves describing the seed nest
Source: Own compilation.

THE MODEL OF APPLE CONTOURS REPRESENTED BY BÉZIER CURVES

Matrix equations for coordinates xAn, yAn, zAn (Fig. 4) of Bézier curve points for the upper part of the apple – A are as follows:

$$xAn_t = Ax \cdot \left[1 - \frac{t}{N}\right]^3 + Anx \cdot \cos\left(\frac{\alpha n \cdot \pi}{180}\right) \cdot 3\frac{t}{N} \cdot \left[1 - \frac{t}{N}\right]^2 +$$

$$+ AAnx \cdot \cos\left(\frac{\alpha n \cdot \pi}{180}\right) \cdot 3 \cdot \left[\frac{t}{N}\right]^2 \cdot \left[1 - \frac{t}{N}\right] + ABnx \cdot \cos\left(\frac{\alpha n \cdot \pi}{180}\right) \cdot \left[\frac{t}{N}\right]^3 \tag{1}$$

$$yAn_t = Ay \cdot \left[1 - \frac{t}{N}\right]^3 + Any \cdot \sin\left(\frac{\alpha n \cdot \pi}{180}\right) \cdot 3\frac{t}{N} \cdot \left[1 - \frac{t}{N}\right]^2 +$$

$$+ AAny \cdot \sin\left(\frac{\alpha n \cdot \pi}{180}\right) \cdot 3 \cdot \left[\frac{t}{N}\right]^2 \cdot \left[1 - \frac{t}{N}\right] + ABny \cdot \sin\left(\frac{\alpha n \cdot \pi}{180}\right) \cdot \left[\frac{t}{N}\right]^3 \tag{2}$$

$$zAn_t = Az \cdot \left[1 - \frac{t}{N}\right]^3 + Anz \cdot 3\frac{t}{N} \cdot \left[1 - \frac{t}{N}\right]^2 + AAnz \cdot 3 \cdot \left[\frac{t}{N}\right]^2 \cdot \left[1 - \frac{t}{N}\right] + ABnz \cdot \left[\frac{t}{N}\right]^3 \tag{3}$$

Matrix equations for coordinates xBn, yBn, zBn (Fig. 4) of Bézier curve points for the middle part of the apple – B are as follows:

$$xBn_t = ABnx \cdot \cos\left(\frac{\alpha n \cdot \pi}{180}\right) \cdot \left[1 - \frac{t}{N}\right]^3 + Bnx \cdot \cos\left(\frac{\alpha n \cdot \pi}{180}\right) \cdot 3\frac{t}{N} \cdot \left[1 - \frac{t}{N}\right]^2 +$$

$$+ BBnx \cdot \cos\left(\frac{\alpha n \cdot \pi}{180}\right) \cdot 3 \cdot \left[\frac{t}{N}\right]^2 \cdot \left[1 - \frac{t}{N}\right] + BCnx \cdot \cos\left(\frac{\alpha n \cdot \pi}{180}\right) \cdot \left[\frac{t}{N}\right]^3 \tag{4}$$

$$yBn_t = ABny \cdot \left[1 - \frac{t}{N}\right]^3 + Bny \cdot \sin\left(\frac{\alpha n \cdot \pi}{180}\right) \cdot 3\frac{t}{N} \cdot \left[1 - \frac{t}{N}\right]^2 +$$

$$+ BBny \cdot \sin\left(\frac{\alpha n \cdot \pi}{180}\right) \cdot 3 \cdot \left[\frac{t}{N}\right]^2 \cdot \left[1 - \frac{t}{N}\right] + BCny \cdot \sin\left(\frac{\alpha n \cdot \pi}{180}\right) \cdot \left[\frac{t}{N}\right]^3 \tag{5}$$

$$zBn_t = ABnz \cdot \left[1 - \frac{t}{N}\right]^3 + Bnz \cdot 3\frac{t}{N} \cdot \left[1 - \frac{t}{N}\right]^2 + BBnz \cdot 3 \cdot \left[\frac{t}{N}\right]^2 \cdot \left[1 - \frac{t}{N}\right] + BCnz \cdot \left[\frac{t}{N}\right]^3 \tag{6}$$

Matrix equations for coordinates *xCn*, *yCn*, *zCn* (Fig. 4) of Bézier curve points for the lower part of the apple – C are as follows:

$$xCn_t = BCnx \cdot \cos\left(\frac{\alpha n \cdot \pi}{180}\right) \cdot \left[1 - \frac{t}{N}\right]^3 + CCnx \cdot \cos\left(\frac{\alpha n \cdot \pi}{180}\right) \cdot 3\frac{t}{N} \cdot \left[1 - \frac{t}{N}\right]^2 +$$

$$+ Cnx \cdot \cos\left(\frac{\alpha n \cdot \pi}{180}\right) \cdot 3 \cdot \left[\frac{t}{N}\right]^2 \cdot \left[1 - \frac{t}{N}\right] + Cx \cdot \left[\frac{t}{N}\right]^3 \tag{7}$$

$$yCn_t = BCny \cdot \sin\left(\frac{\alpha n \cdot \pi}{180}\right) \cdot \left[1 - \frac{t}{N}\right]^3 + CCny \cdot \sin\left(\frac{\alpha n \cdot \pi}{180}\right) \cdot 3\frac{t}{N} \cdot \left[1 - \frac{t}{N}\right]^2 +$$

$$+ Cny \cdot \sin\left(\frac{\alpha n \cdot \pi}{180}\right) \cdot 3 \cdot \left[\frac{t}{N}\right]^2 \cdot \left[1 - \frac{t}{N}\right] + Cy \cdot \left[\frac{t}{N}\right]^3 \tag{8}$$

$$zCn_t = BCnz \cdot \left[1 - \frac{t}{N}\right]^3 + CCnz \cdot 3\frac{t}{N} \cdot \left[1 - \frac{t}{N}\right]^2 + Cnz \cdot 3 \cdot \left[\frac{t}{N}\right]^2 \cdot \left[1 - \frac{t}{N}\right] + Cz \cdot \left[\frac{t}{N}\right]^3 \tag{9}$$

For $N = 23$, $t = 0, \ldots, N$, n – the Bézier curve number, $n = 1, 2, 3, \ldots, 10$. On the basis of three connected Bézier curves, an apple contour is obtained (Fig. 5). Bézier curves are connected at nodal points. In order to ensure smoothness of connection of curves at nodal points, the condition of control points of the curves being connected being positioned within a plane and a joint straight line, has been met. On the basis of equations 1 to 9, it is possible to develop 30 Bézier curves along the apple meridians, making up its 3D model. There are 23 points on each curve.
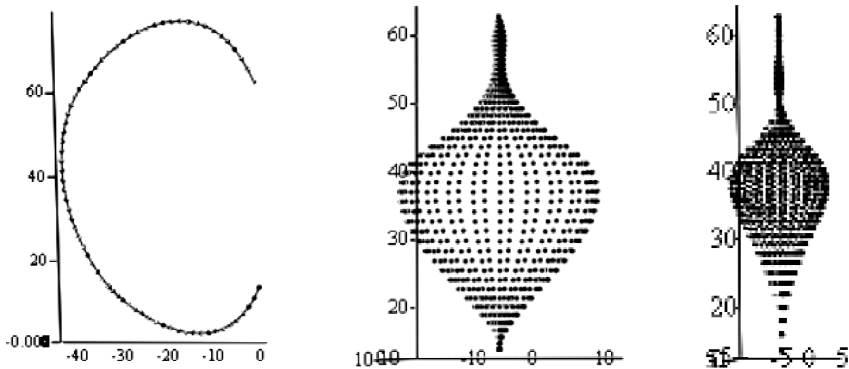

FIGURE 5. An example of three Bézier curves connected for the apple contour and two Bézier curves connected for the contours of the seeds the chamber and seed nest
Source: Own compilation.

APPLE SEEDS THE CHAMBER AND SEED NEST MODELS REPRESENTED BY BÉZIER CURVES

Matrix equations for coordinates $xAk1$, $zAk1$ of the points of the first Bézier curve for the seeds the chamber are as follows:

$$xAk1_{t1} = Ax \cdot \left[1 - \frac{t1}{N}\right]^3 + Ak1x \cdot 3\frac{t1}{N} \cdot \left[1 - \frac{t1}{N}\right]^2 + Bk1x \cdot 3 \cdot \left[\frac{t1}{N}\right]^2 \cdot \left[1 - \frac{t1}{N}\right] + Bkx \cdot \left[\frac{t1}{N}\right]^3$$

(10)

$$zAk1_{t1} = Az \cdot \left[1 - \frac{t1}{N}\right]^3 + Ak1z \cdot 3\frac{t1}{N} \cdot \left[1 - \frac{t1}{N}\right]^2 + Bk1z \cdot 3 \cdot \left[\frac{t1}{N}\right]^2 \cdot \left[1 - \frac{t1}{N}\right] + Bkz \cdot \left[\frac{t1}{N}\right]^3$$

(11)

Matrix equations for coordinates $xAk2$, $zAk2$ of the points of the second Bézier curve for the seeds the chamber are as follows:

$$xAk2_t = Bkx \cdot \left[1 - \frac{t}{N}\right]^3 + Bk2x \cdot 3\frac{t}{N} \cdot \left[1 - \frac{t}{N}\right]^2 + Ck1x \cdot 3 \cdot \left[\frac{t}{N}\right]^2 \cdot \left[1 - \frac{t}{N}\right] + Cx \cdot \left[\frac{t}{N}\right]^3$$

(12)

$$zAk2_t = Bkz \cdot \left[1 - \frac{t}{N}\right]^3 + Bk2z \cdot 3\frac{t}{N} \cdot \left[1 - \frac{t}{N}\right]^2 + Ck1z \cdot 3 \cdot \left[\frac{t}{N}\right]^2 \cdot \left[1 - \frac{t}{N}\right] + Cz \cdot \left[\frac{t}{N}\right]^3$$

(13)

In order to obtain a rotational solid representing the seeds the chamber, the first Bézier curve (equations 10, 11) and then the second Bézier curve (equations 12, 13) were rotated:

$$XAk1_{t1, j} = xAk1_{t1} \cdot \sin(\phi_j)$$

(14)

$$YAk1_{t1, j} = xAk1_{t1} \cdot \cos(\phi_j)$$

(15)

$$ZAk1_{t1, j} = zAk1_{t1}$$

(16)

$$XAk2_{t, j} = xAk2_t \cdot \sin(\phi_j)$$

(17)

$$YAk2_{t, j} = xAk2_t \cdot \cos(\phi_j)$$

(18)

$$ZAk2_{t,\,j} = zAk2_t \tag{19}$$

where: $\phi_j = \dfrac{2 \cdot \pi \cdot j}{N}$ \qquad (20)

Range variables for these equations are saved in vector 21:

$$\begin{bmatrix} t \\ j \\ t1 \end{bmatrix} = \begin{bmatrix} 0\ldots N \\ 0\ldots N \\ 0\ldots N-1 \end{bmatrix} \tag{21}$$

Rows of the matrix, obtained on the basis of rotation of Bézier curves, have been connected using the stack procedure:

$$Xka := \mathrm{stack}(XAk1, XAk2) \tag{22}$$

$$Yka := \mathrm{stack}(YAk1, YAk2) \tag{23}$$

$$Zka := \mathrm{stack}(ZAk1, ZAk2) \tag{24}$$

The seed nest shape model has been described in the manner similar to the seeds the chamber. For this purpose, in equations 10 to 23, it is necessary to replace k with g.

SUMMARY

The presented method proposing to use Bézier curves may be used for mathematical modeling of apple shape. The concave and convex parts of the apple can be described using three connected Bézier curves. The basis for description of apple contours using 30 Bézier curves comprises of photographs of the apple rotated every 36° with reference to its natural axis of symmetry. Bézier curves along the apple's meridians constitute its 3D model. There are 690 points on the apple model surface. Using two connected Bézier curves, upon their rotation with reference to the longitudinal axis of symmetry of the apple, it is possible to describe the shape of the seeds the chamber and seed nest of the fruit.

REFERENCES

ABERA M.K., VERBOVEN P., HERREMANS E., DEFRAEYE T., FANTA S.W., HO Q.T., CARMELIET J., NICOLAĎ B.M. 2014: 3D Virtual Pome Fruit Tissue Generation Based on Cell Growth Modeling. Food Bioprocess Technology 7: 542–555.

ANDERS A., MARKOWSKI P., KALINIE-WICZ Z. 2014: Badanie właściwości geometrycznych i fizycznych owoców wybranych odmian gruszy na podstawie modeli numerycznych uzyskanych za pomocą skanera 3*D*. Zeszyty Problemowe Postępów Nauk Rolniczych 577: 3–12.

ARSHAD M., SHAHNAWAZ M., SHAHKEELA S., HUSSAIN M., AHMAD M., KHAN S.S. 2014: Significance of physical properties of apple fruit influenced by preharvest orchard management factors. European Journal of Experimental Biology 4 (5): 82–89.

BAKANE P.H., REDDY R.B., KHEDKAR M.B. 2014: Physical Properties of Custard Apple (*Annona squamosa*) Seeds. Periodic Research RNI No. UPBIL/2012/55438, III, I: 252–254.

BULIŃSKI J., WASZKIEWICZ Cz., BURA-CZEWSKI P. 2012: Stock management as an element of enterprise strategy. Annals of Warsaw University of Life Sciences – SGGW, Agriculture (Agricultural and Forest Engineering) 60: 137–148.

BULIŃSKI J., WASZKIEWICZ Cz., BURA-CZEWSKI P. 2013: Utilization of ABC/XYZ analysis in stock planning in the enterprise. Annals of Warsaw University of Life Sciences – SGGW, Agriculture (Agricultural and Forest Engineering) 61: 89–96.

CHAKESPARI A.G., RAJABIPOUR A., MOB-LI H. 2010: Mass modeling of two apple varieties by geometrical attributes. Australian Journal Agricultural Engineering 1 (3): 112–118.

COSTA C., ANTONUCCI F., PALLOTTINO F., AGUZZI J., SUN D.-W., MENESATTI P. 2011: Shape analysis of agricultural products: a review of recent research advances and potential application to computer vision. Food and Bioprocess Technology 4: 673–692.

FOLEY J.D., Van DAM A., FEINER S.K., HUGHES J.F., PHILLIPS R.L. 2001: Wprowadzenie do grafiki komputerowej. WNT, Warszawa.

GOŃI S.M., PURLIS E. 2010: Geometric modelling of heterogeneous and complex foods. Journal of Food Engineering 372, 97(4): 547–554.

GOŃI S.M., PURLIS E., SALVADORI V.O. 2008: Geometry modelling of food materials from magnetic resonance imaging. Journal of Food Engineering 88: 561–567.

HAZBAVI A.I. 2014: Maximum Height Calculation for Bulk of Apple Fruits (var. Golden Delicious). Journal of Agroalimentary Processes and Technologies 20 (1): 33–38.

HO Q.T., CARMELIET J., DATTA A.K., DE-FRAEYE T., DELELE M.A., HERREMANS E., OPARA L., RAMON H., TIJSKENS E., van der SMAN R., Van LIEDEKERKE P., VERBOVEN P., NICOLAI B.M. 2013: Multiscale modeling in food engineering. Journal of Food Engineering 114 (3): 279–291.

JANASZEK M., TRAJER J. 2010: Classification system as diagnostics tool for the plant products. Annals of Warsaw University of Life Sciences – SGGW, Agriculture (Agricultural and Forest Engineering) 56: 51–56.

KAKADIYA D., SHAH R., SHAH N., KA-CHARIYA C., PATEL M., SUKHWANI K. 2015: Shape Extraction Methods for Fruits: Technical Review. International Journal of Computer Applications 111 (1): 43–48.

KICIAK P. 2000: Podstawy modelowania krzywych i powierzchni. Zastosowania w grafice komputerowej. WNT, Warszawa.

LIMING X., YANCHAO Z. 2010: Automated strawberry grading system based on image processing. Computers and Electronics in Agriculture 71: 32–39.

MEBATSION H.K., BOUDON F., GODIN C., PRADAL C., GÉNARD M., GOZ-BAC C., BERTIN N. 2011: A novel profile based model 415 for virtual representation of quasi-symmetric plant organs. Computers and Electronics in Agriculture 75 (1), 113–124.

MOREDA G.P., MUŃOZ M.A., RUIZ-ALTI-SENT M., PERDIGONES A. 2012: Shape determination of horticultural produce using two-dimensional computer vision – A review. Journal of Food Engineering 108 (2), 245–261.

PANDEY R., NAIK S., MARFATIA R. 2013: Image Processing and Machine Learning for Automated Fruit Grading System: A Technical Review. International Journal of Computer Applications 81 (16): 29–39.

PRUSINKIEWICZ P., RUNIONS A. 2012: Computational models of plant development and form. New Phytologist 193 (3), 431; 549–569.

ROGGE S., BEYENE S.D, HERREMANS E., HERTOG M.L., DEFRAEYE T., VERBOVEN P., NICOLAI B.M. 2014: A geometrical model generator for quasi – axisymmetric biological products. Food Bioprocess Technology 7: 1783–1792. DOI 10.1007/s11947-013-1169-6.

TORABI A., TABATABAEKOLOOR R., HASHEMI S.J. 2013: Volume Modelling of Three Apple Varieties Based on Physical Parameters. International Journal of Agriculture and Food Science Technology 4, 5: 461–466.

UYAR R., ERDOĐDU F. 2009: Potential use of 3-dimensional scanners for food process modeling. Journal of Food Engineering 93: 337–343.

Streszczenie: *Metoda rekonstrukcji 3D kształtu jabłek. Cz. 1. Metoda matematycznego modelowania kształtu jabłek*. W niniejszej pracy przedstawiono propozycję metody matematycznego modelowania kształtu jabłek z wykorzystaniem krzywych Béziera. Kontur jabłka leżący na jego południku opisano trzema połączonymi krzywymi Béziera. Podstawą do opisu konturów jabłka za pomocą krzywych Béziera są uzyskane fotografie z obracanego co 36° jabłka względem

jego naturalnej osi symetrii. Krzywe Béziera roz-
mieszczono wzdłuż południków jabłka, stanowią
jego model 3D. Za pomocą krzywych Béziera
opisano kształty komory nasiennej i gniazda na-
siennego jabłka.

Authors' address:
Leszek Mieszkalski
Wydział Inżynierii Produkcji SGGW
Katedra Organizacji i Inżynierii Produkcji
02-787 Warszawa, ul. Nowoursynowska 164
Poland
e-mail: leszek_mieszkalski@sggw.pl